Plasma Membrane H^+-ATPase Is Involved in Auxin-Mediated Cell Elongation during Wheat Embryo Development[1]

Nicole Rober-Kleber, Jolana T.P. Albrechtová, Sonja Fleig, Norbert Huck[2], Wolfgang Michalke, Edgar Wagner, Volker Speth, Gunther Neuhaus, and Christiane Fischer-Iglesias*

Institute for Biology II, Department of Cell Biology, Albert-Ludwigs-University of Freiburg, Schänzlestrasse 1, 79104 Freiburg, Germany (N.R.-K., J.T.P.A., S.F., N.H., E.W., V.S., G.N., C.F.-I.); and Institute for Biology III, Albert-Ludwigs-University of Freiburg, 79104 Freiburg, Schänzlestrasse 1, Germany (W.M.)

Previous investigations suggested that specific auxin spatial distribution due to auxin movements to particular embryonic regions was important for normal embryonic pattern formation. To gain information on the molecular mechanism(s) by which auxin acts to direct pattern formation in specific embryonic regions, the role of a plasma membrane (PM) ATPase was evaluated as downstream target of auxin in the present study. Western-blot analysis revealed that the PM H^+-ATPase expression level was significantly increased by auxin in wheat (*Triticum aestivum*) embryos (two–three times increase). In bilaterally symmetrical embryos, the spatial expression pattern of the PM H^+-ATPase correlates with the distribution pattern of the auxin analog, tritiated 5-azidoindole-3-acetic acid. A strong immunosignal was observed in the abaxial epidermis of the scutellum and in the epidermal cells at the distal tip of this organ. Pseudoratiometric analysis using a fluorescent pH indicator showed that the pH in the apoplast of the cells expressing the PM H^+-ATPase was in average more acidic than the apoplastic pH of nonexpressing cells. Cellulose staining of living embryos revealed that cells of the scutellum abaxial epidermis expressing the ATPase were longer than the scutellum adaxial epidermal cells, where the protein was not expressed. Our data indicate that auxin activates the proton pump resulting in apoplastic acidification, a process contributing to cell wall loosening and elongation of the scutellum. Therefore, we suggest that the PM H^+-ATPase is a component of the auxin-signaling cascade that may direct pattern formation in embryos.

In recent years, evidence was provided that auxin plays an important role in embryonic pattern formation of monocots and dicots. Investigation of embryo morphogenesis by perturbing in vitro development of young wheat (*Triticum aestivum*) embryos with exogenous auxin and auxin transport inhibitors led to the formation of specific abnormal embryos. Morphological alterations were ranging from complete failure of the establishment of bilateral symmetry to abnormal overall bilateral symmetry or differentiation of supernumerary meristems and organs (Fischer and Neuhaus, 1996; Fischer et al., 1997). Treatment of zygotic Indian mustard (*Brassica juncea*) embryos with auxins, an antiauxin, and auxin transport inhibitors also induced a variety of phenotypical aberrations. Abnormal embryos were showing a complete blockage of morphogenesis, loss of embryonic organs, or defects in cotyledon separation (Liu et al., 1993; Hadfi et al., 1998). Some of these abnormal *Brassica* spp. embryos phenocopied pattern mutants of Arabidopsis such as *shoot meristemless*, *gnom*, *fackel*, *monopteros*, and *gurke* (Jürgens et al., 1991; Mayer et al., 1991, 1993; Berleth and Jürgens, 1993; Endrizzi et al., 1996; Torres-Ruiz et al., 1996). Finally, exogenous auxins and auxin transport inhibitors have also profound effects on the development of carrot (*Daucus carota*) somatic embryos (Schiavone and Cooke, 1987).

Because auxin transport inhibitors disrupt normal embryogenesis, it has been suggested that specific auxin spatial distribution due to auxin movements to particular embryonic regions may be important in establishing normal embryonic pattern formation (Fischer and Neuhaus, 1996; Fischer et al., 1997). The distribution of an analog of indole-3-acetic acid (IAA), the photoaffinity labeling agent, tritiated 5-azidoindole-3-acetic acid ([^{3}H],5-N_3IAA) was visualized in zygotic wheat embryos and was used to deduce auxin transport pathways in these embryos (Fischer-Iglesias et al., 2001). This study showed that distribution of azido-auxin is heterogeneous and changes during embryo development. In particular, the shift from radial to bilateral symmetry was correlated with a redistribution of [^{3}H],5-N_3IAA in the embryo probably achieved by active polar transport to specific embryonic regions (Fischer-Iglesias et al., 2001).

The molecular basis of auxin response is still poorly understood. A combination of genetic and

[1] This work was supported by the Deutsche Forschungsgemeinshaft (grant no. SFB 592).

[2] Present address: Department of Plant Biology, University of Zürich, Zollikerstrasse 107, CH–8008 Zürich, Switzerland.

* Corresponding author; e-mail Fischer_Iglesias@hotmail.com; fax 49–761–203–26–75.

Article, publication date, and citation information can be found at www.plantphysiol.org/cgi/doi/10.1104/pp.013466.

molecular approaches led recently to a model in which auxin signaling is mediated by regulated protein degradation (for review, see Ward and Estelle, 2001; Guilfoyle and Hagen, 2001). In brief, *Aux/IAA* genes encode short-lived nuclear proteins that repress auxin-regulated gene expression through interaction with the ARF family of transcription factors (Ulmasov et al., 1997b). Auxin response factors (ARFs) have been shown to bind to auxin response elements found in promoters of early auxin response genes (Ulmasov et al., 1997a). Studies of two ARFs, IAA24/ARF5 (MONOPTEROS), ARF3 (ETTIN), and a Aux/IAA (BODENLOS) provide evidence for a link between auxin action and pattern formation (Sessions et al., 1997; Hardtke and Berleth, 1998; Hamann et al., 2002). It has recently been shown that MONOPTEROS and BODENLOS interact in two hybrid assays suggesting that BODENLOS inhibits MONOPTEROS action in root meristem initiation (Hamann et al., 2002). It has been proposed that Aux/IAA proteins are targeted for degradation by the ubiquitin-ligase complex (E3) known as SCF^{TIR1} thus releasing the ARF proteins to activate downstream transcription of early response genes involved in auxin-mediated growth and development (Gray et al., 1999; Ward and Estelle, 2001). It has also been proposed that auxin acts to regulate the phosphorylation of Aux/IAA proteins and thereby mark them for degradation (Leyser, 2001; Reed, 2001). A MAP kinase and a Ser-Thr kinase called PINOID have been shown to negatively regulate auxin signaling and therefore have been proposed as possible candidates to phosphorylate Aux/IAAs (Kovtun et al., 1998; Christensen et al., 2000). In recent years, much attention has been focused on the identification of the components of the SCF^{TIR1} degradation pathway (Del Pozo et al., 1998; Ruegger et al., 1998; Lyapina et al., 2001; Schwechheimer et al., 2001).

The molecular mechanisms by which auxin acts to direct morphogenesis in specific regions of the embryo are still poorly understood. Therefore gaining information on these processes and identifying downstream targets of auxin in the signal transduction pathway that directs pattern formation in embryos are the aims of the present study. We evaluated the role of a plasma membrane (PM) H^+-ATPase as component of this auxin-signaling cascade. Plant PM H^+-ATPases are electrogenic proton pumps that play a major role in the control of various cell processes. Using ATP as energy source, the enzyme pumps protons from the cytoplasm to the cell exterior, thus creating an electrochemical gradient across the PM that constitutes the driving force for nutrient uptake. For example, Suc uptake by broad bean (*Vicia faba*) embryos is an H^+-cotransport process energized by the gradients created by the PM H^+-ATPase (El Ayadi, 1987; Bouche-Pillon et al., 1994). Extensive acidification of the apoplast is also believed to contribute to cell wall loosening, a prerequisite for cell growth (Rayle and Cleland, 1992; Kutschera, 2001). Molecular cloning has demonstrated the existence of several genes expressing similar but distinct forms of the proton pump (Ewing and Bennett, 1994; Sussman, 1994). Regulation of the PM H^+-ATPase is achieved by important factors controlling plant physiology such as hormones, environmental stresses, phytohormones, phytotoxins, and light (Serrano, 1989). In particular, several studies showed that auxin specifically increased the level of PM H^+-ATPase by a factor of two to three times in elongating tissues such as maize (*Zea mays*) coleoptiles (Hager et al., 1991; Frias et al., 1996).

In the present study, we determined whether PM H^+-ATPase protein was regulated by auxin in wheat embryos. By means of immunolocalization approach, the spatial distribution of the enzyme has been investigated in normal embryos at different developmental stages as well as in abnormal embryos in which auxin distribution or levels were altered. Special attention was devoted to reveal correlations between the distribution pattern of photolytically fixed analog of IAA (Fischer-Iglesias et al., 2001) and the expression pattern of the PM-ATPase. Finally, we investigated whether cell wall acidification followed by cell elongation occurred in the cells in which the PM-ATPase was expressed.

RESULTS

Induction of ATPase Protein Expression by Auxin in Wheat Embryos

Detection of PM H^+-ATPase in wheat embryos was performed using the specific monoclonal antibody 46E5B11, originally raised against corn PM H^+-ATPase (Villalba et al., 1991; Jahn et al., 1998). This antibody also specifically recognizes PM H^+-ATPase(s) of *Elodea canadensis*, another monocotyledon (Baur et al., 1996) and three isoforms of PM H^+-ATPase in Arabidopsis (Palmgren and Christensen, 1994). In the present study, a band having a size of approximately 100 kD, characteristic for higher plant PM H^+-ATPase was detected by this monoclonal antibody in PM-enriched microsomal vesicles of corn, Arabidopsis, and wheat (Fig. 1A). A band of this size was also detected specifically in total protein extracts of wheat embryos (Fig. 1B). A significant increase of the ATPase protein level was observed in excised embryos treated in vitro with 30 μM IAA for 2 h compared with control embryos, incubated in buffer without IAA (Fig. 1B).

Immunolocalization of PM H^+-ATPase Protein in Wheat Embryos at Different Developmental Stages

In globular embryos, only the cells of the suspensor were immunostained whereas no signal was detected in cells of the embryo proper (Fig. 2A). In bilaterally symmetrical embryos, regardless of the developmen-

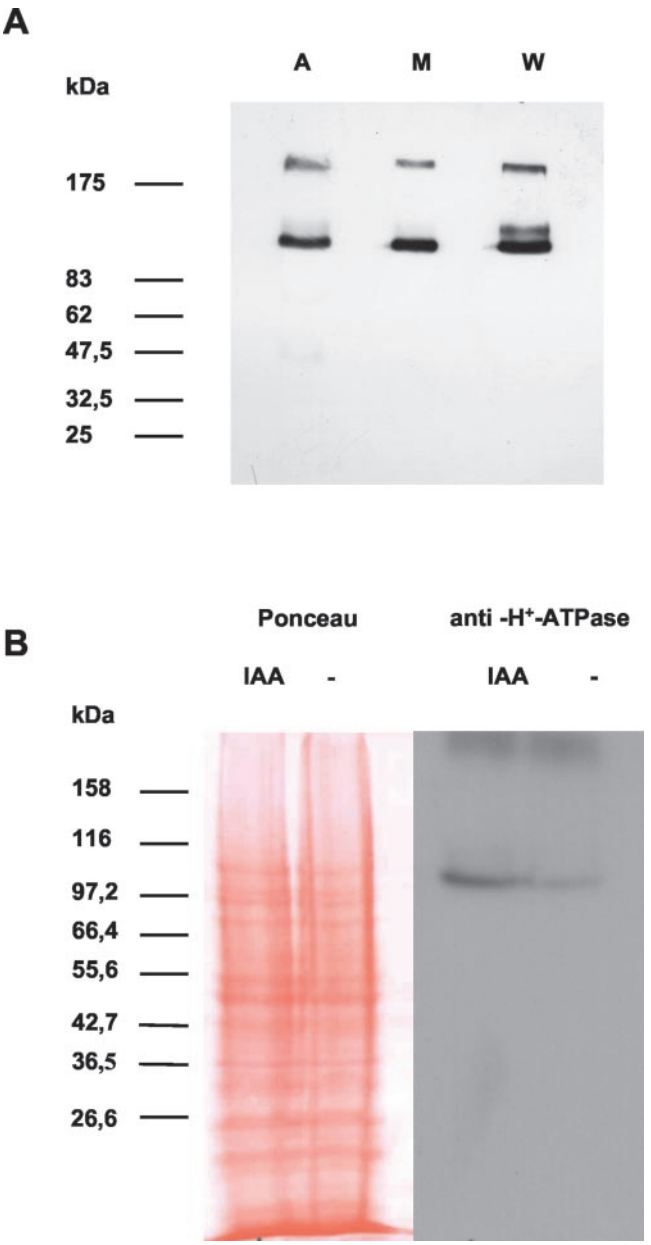

Figure 1. Effect of IAA on the level of PM H^+-ATPase antigen in wheat embryos. A, PM-enriched microsomal preparations of Arabidopsis (A), maize (M), and wheat (W) probed with the monoclonal antibody 46 E5B11. B, Left panel, Gel blot of protein extracts from IAA-treated and untreated embryos. Equal amounts of total protein extracts were separated by electrophoresis on SDS-PAGE gels and stained by Ponceau Red. Right panel, Western-blot analysis of total protein extracts from embryos incubated for 2 h either on Murashige and Skoog medium supplemented with 30 μM IAA or on auxin-free Murashige and Skoog medium. Detection of the PM H^+-ATPase was performed using the specific monoclonal antibody 46E5B11.

tal stage observed, the suspensor always showed a strong immunostaining (Fig. 2, B–E). In transition embryos, immunosignal was specifically observed in the epidermal and subepidermal cells of the scutellum (Fig. 2B). In older bilaterally symmetrical embryos grown in planta and in vitro, a strong signal was observed in the abaxial epidermis of the scutellum and in the adaxial epidermal cells at the distal tip of this organ (Figs. 2E and 3A). A weaker immunostaining was also detected in the respective subepidermal cells (Figs. 2E and 3A). In contrast, no significant ATPase expression was detected in the lower part of the adaxial scutellar epidermis, in the shoot and root meristems, leaf primordia, and coleoptile (Figs. 2E and 3A). Immunogold staining of the H^+-ATPase in abaxial epidermal cells of the scutellum showed that the protein was localized to the PM (Fig. 2F).

In bilaterally symmetrical embryos, the spatial expression pattern of the PM H^+-ATPase correlated with the distribution pattern of the auxin analog [^{3}H],5-N_3IAA. The cells showing the strongest immunosignal were also those having the highest tritium activity (Fig. 2, B–E; Fig. 1 in Fischer-Iglesias et al., 2001). In particular, besides suspensor cells, [^{3}H],5-N_3IAA was found to be most abundant in the epidermis of the scutellum of transition embryos, whereas in older bilaterally symmetrical embryos, the highest activity was detected in the abaxial epidermis of the scutellum and in the adaxial epidermal cells at the tip of this organ (Fischer-Iglesias et al., 2001). However, in radially symmetrical embryos, although the auxin analog was observed in all protodermal cells around the embryo proper (Fig. 1 in Fischer-Iglesias et al., 2001), no ATPase expression was detected in these cells (Fig. 2A).

Localization of H^+-ATPase Protein in Morphologically Abnormal Embryos

To investigate whether the spatial distribution pattern of H^+-ATPase protein varies in correlation with altered distribution or concentration of auxin, immunolocalization of the protein was performed on zygotic wheat embryos excised at the globular stage and grown on media supplemented with auxin and auxin transport inhibitors.

Treatment with the transport inhibitor *N*-1-naphthylphthalamic acid leads to the differentiation of multiple meristems (shoot and root meristems) and multiple organs (coleoptiles and scutella; Fischer et al., 1997). One representative category of these embryos called "back to back" Siamese embryos has been analyzed. In these embryos, a strong immunostaining was observed in the epidermal and subepidermal cells of the two fused scutella oriented in opposite directions, in the suspensor and in the cells of the proximal embryonic region (Fig. 3B). No significant expression of ATPase protein was observed in the shoot meristems (Fig. 3B).

In the presence of TIBA belonging to another auxin transport inhibitor family, globular zygotic embryos developed an overall abnormal bilateral symmetry such that the shoot apical meristem was shifted to the

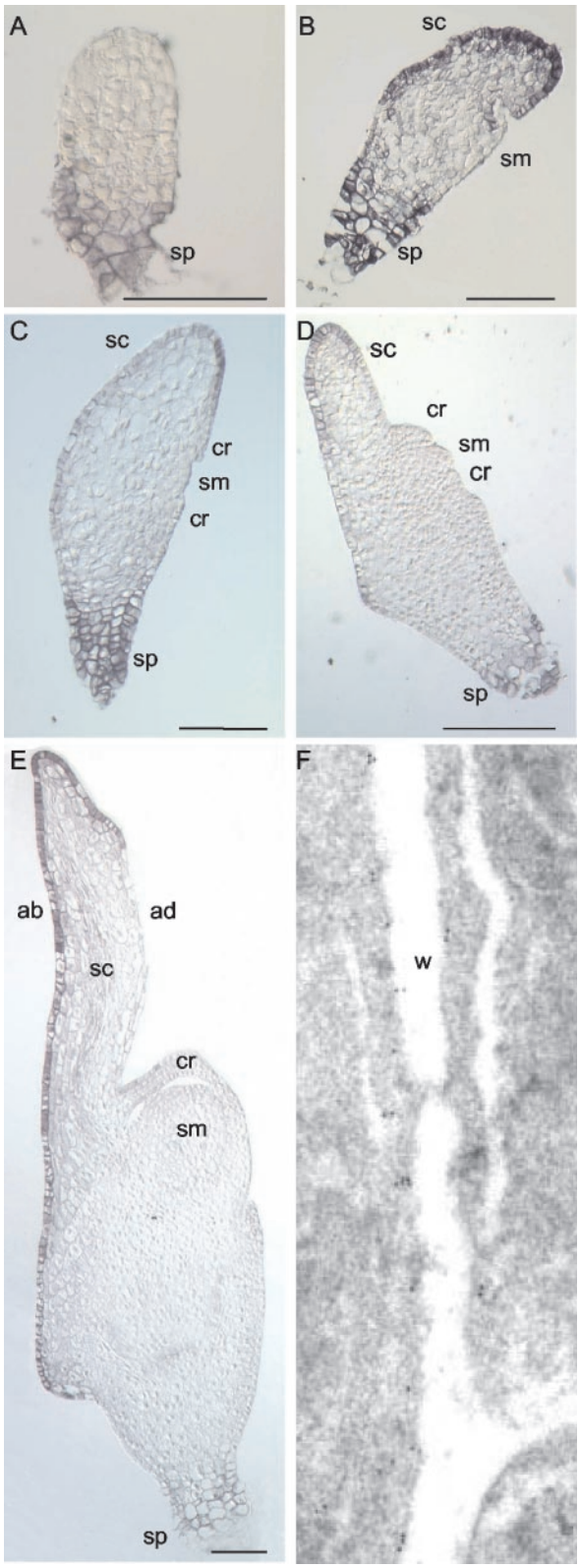

Figure 2. Immunolocalization of PM H^+-ATPase in wheat embryos at different developmental stages. A, Globular embryo; B, late transition stage; C, early coleoptilar stage; D, late coleoptilar stage/early "stage 1"; E, fully differentiated immature embryo. F, Immunogold staining of the H^+-ATPase in epidermal cells of the scutellum (walls in between epidermal and subepidermal cell layers). ab, Abaxial; ad, adaxial; cr, coleoptilar ring; sc, scutellum; sm, shoot meristem; sp, suspensor; w, cell wall; bars in A through E = 100 μm; magnification in F, 25,000×.

upper part of the embryo due to cell elongation and to excessive cell division between the shoot meristem and the suspensor (Fischer and Neuhaus, 1996). Differentiation of the scutellum and the shoot meristem were altered, and the embryonic root was missing. TIBA-treated embryos showed strong ATPase protein expression in the suspensor and the elongation area between the shoot meristem and the scutellum (Fig. 3C). A relatively strong expression was observed in the epidermal scutellar cells. Finally, the subepidermal cells of the scutellum were also decorated (Fig. 3C). In contrast, no significant expression of ATPase protein was detected in the abnormal shoot meristem (Fig. 3C).

Globular embryos grown on media supplemented with exogenous auxins such as 2,4,5-trichlorophenoxy-acetic acid (2,4,5-T) were not able to undergo the shift to bilateral symmetry (Fischer and Neuhaus, 1996). An increase of size of the embryo proper was observed due to continuous radial growth ("radial growth" phenotype). Early transition embryos that had already initiated differentiation of their scutellum and their shoot meristem before 2,4,5-T was added developed a rounded scutellum and a abnormal protruding shoot meristem ("arrested growth" phenotype; Fischer and Neuhaus, 1996). The suspensor and the proximal region of such embryos always showed high expression levels of H^+-ATPase (Fig. 3, D–F). In radial growth embryos, high ATPase levels were observed in all epidermal and subepidermal cells around the radial embryo proper (Fig. 3, D and E). In arrested growth embryos, a stronger immunosignal was detected in the epidermal and subepidermal cells of the rounded scutellum compared with the immunostaining observed in the abnormal shoot meristem (Fig. 3F). An immunosignal whose intensity ranged from relatively high to high was observed in the inner cell layers of the rounded distal part of most embryos regardless of whether they had differentiated a shoot apical meristem (Fig. 3, D–F).

Comparison of H^+-ATPase expression pattern with azido-auxin distribution pattern in the different types of morphologically abnormal embryos observed showed that the cells that contained significant amounts of [^{3}H],5-N_3IAA (Figs. 4 and 5 in Fischer-Iglesias et al., 2001) also expressed significantly the H^+-ATPase (Fig. 3).

Pseudoratiometric Measurements of Cell Wall pH

To test whether the localized expression of H^+-ATPase correlates with acidification of cell walls, confocal ratio imaging was used to measure apoplastic pH in two selected areas of the scutellum (Fig. 4).

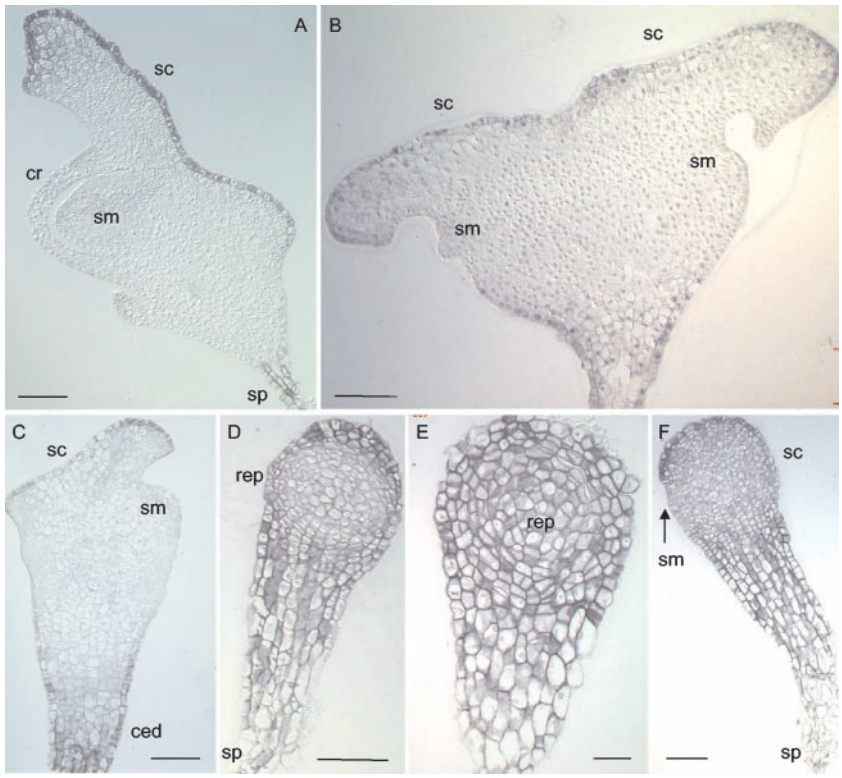

Figure 3. Immunolocalization of PM H^+-ATPase in wheat embryos treated with auxin and different auxin transport inhibitors in vitro. A, Normal in vitro grown embryo; B, embryo isolated at the globular stage and grown on media supplemented with *N*-1-naphthylphthalamic acid; C, abnormal embryo induced by treatment on media supplemented with 2,3,5-triiodobenzoic acid (TIBA); D and E, radial growth phenotypes observed on media supplemented with 2,4,5-T; F, arrested growth phenotype observed on media supplemented with 2,4,5-T. ced, Area of cell elongation and division; cr, coleoptilar ring; rep, rounded embryo proper; sc, scutellum; sm, shoot meristem; sp, suspensor; bars = 100 μm.

Adaxial epidermal cells at the scutellar tip in area 1 were monitored as PM H^+-ATPase-expressing cells (Figs. 2, D and E, and 4B). Area 2, consisting of scutellar adaxial epidermal cells close to the coleoptilar ring, was chosen as the nonexpressing PM-H^+ATPase reference area (Figs. 2, D and E, and 4B). The cell wall pH was determined by pseudoratio imaging, which is monitoring the pH-sensitive fluorescence of Oregon Green (OG) and comparing it with the pH-insensitive fluorescence of Texas Red (TR) used as internal control. Dextran-conjugated dyes OG and TR were added to the culture medium of the embryos at a concentration of 80 and 300 μM, respectively. As expected due to their large M_r and charge properties, the dyes were membrane impermeable, and no obvious dye penetration into the cytoplasma was found. Significant dye leakage from the embryos was observed only after more than 45 min of incubation in the dye-free solution (data not shown).

Measurements of apoplastic pH were performed on embryos whose first leaf primordium covered the shoot meristem. In younger embryos, retention of the dyes in the cell walls was insufficient and the cell walls were too thin to allow appropriate measurements. Older embryos were not monitored because their pattern formation was almost completed.

Calibration of OG to TR ratio to wall pH was performed by incubating frozen/thawed embryos for 75 min in the culture medium supplemented with the dextran-conjugated dyes and buffered either with 25 mM MES to a pH range of 5.3 to 6.5 or with 25 mM citrate to pHs ranging from 3.6 to 4.7. These measurements from dead embryos were made to assess the responsiveness of the dyes in the wall environment isolated from potential effects of the living embryo cells. The ratio of OG to TR was found to be linearly dependent on the pH in the range of 4.2 to 6.4 (Fig. 4A). Therefore, this approach was valid for monitoring changes in wall pH along the epidermis of the scutellum.

For measurements, the embryos were incubated for 1 h either in the culture medium supplemented with 30 μM IAA or in the culture medium without IAA. The embryos were then transferred for 75 min to fresh culture medium containing the dextran-conjugated dyes, supplemented or not with 30 μM IAA. These measurements indicated that the apoplastic pH at the tip of the scutellum of embryos incubated with IAA was 4.65 (Table I; Fig. 4D), whereas the wall pH of the scutellar epidermal cells closer to the coleoptile was 5.25 (Table I; Fig. 4E). Thus, although both types of cells had a relatively low apoplastic pH, the walls of cells expressing the ATPase were clearly more acidic than those of cells not expressing the enzyme as confirmed by the Student's *t* test ($P = 1.6 \times 10^{-22}$). Apoplastic pH was also determined for embryos that were not incubated in IAA. In this case, the apoplastic pH of cells located at the tip of the scutellum was 5.5 (Table I), whereas the wall pH of the epidermal cells closer to the coleoptile was 5.75 (Table I). In this case, no significant pH gradient was observed between the walls of cells expressing the protein and the walls of cells that do

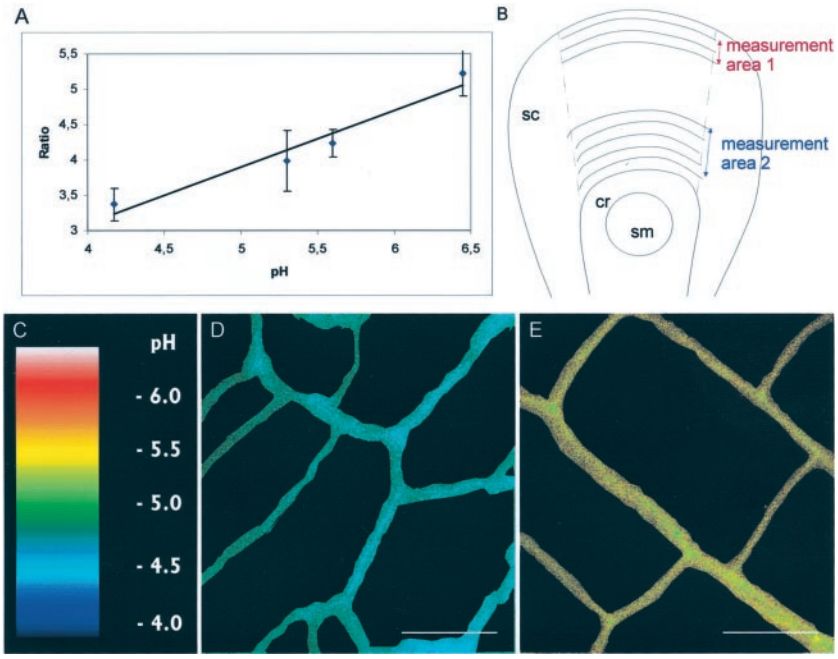

Figure 4. Ratiometric measurements of cell wall pH. A, Calibration of the OG to TR ratio to wall pH. For each pH, 10 to 13 measurements on two to three embryos have been performed. Embryonic stages used for calibration are the same as those used for measurements. B, Areas in which the ratiometric measurements were conducted on the scutellum adaxial epidermis. In area 1, ratios were measured in walls of cells expressing PM H^+-ATPase at the tip of the scutellum. In area 2, ratios were measured in walls of cells not expressing the PM-H^+ATPase near the coleoptilar ring. C, Wall pH has been pseudocolor coded according to the inset scale. D, Representative ratio image of adaxial epidermal cell walls at the tip of the scutellum. E, Representative ratio image of adaxial scutellar epidermal cell walls near the coleoptilar ring. Ratio images in D and E have been processed to subtract the background and to eliminate the fluorescence of the underlying cell walls. Only the cell walls used for evaluation are visible on the photographs. cr, Coleoptilar ring; sc, scutellum; sm, shoot meristem. Bars in D and E = to 10 μm.

not express the ATPase (Student's t test, $P = 0.041$). However, it has to be mentioned that incubation of embryos in a medium without auxin for only 1 h leads to a significant decrease in endogenous IAA level, indicating that IAA is released rapidly from the embryo (Fischer-Iglesias et al., 2001; Table I). Therefore, the "absolute" apoplastic pH value measured at the tip of the scutellum in the latter experimental conditions may not reflect normal in planta situation. However, adding auxin to embryos resulted in a significant acidification of almost 1 pH unit in the cell walls at the tip of the scutellum where the ATPase was expressed (Student's t test, $P = 9.48 \times 10^{-13}$). A weaker acidification of approximately 0.5 pH unit (Student's t test, $P = 3.31 \times 10^{-06}$) was also observed in the walls of the cells near the coleoptilar ring even though neither azido-auxin nor the proton pump was detected in these cells.

Determination of the Cell Size

To determine whether the more acidic apoplastic pH of the cells expressing the ATPase was correlated with a higher elongation activity, the length of the cells of the abaxial scutellum epidermis was compared with the length of the cells of the adaxial scutellar epidermis near the coleoptile (Fig. 5). Two embryonic stages were evaluated, namely bilaterally symmetrical embryos whose first leaf primordium covered approximately one-half of the shoot meristem (middle embryonic stages; Fig. 5A) and slightly older embryos whose first leaf primordium covered the shoot meristem (older embryonic stages; Fig. 5B).

Cellulose staining performed on living embryos of both embryonic stages revealed that the abaxial epidermal cells were significantly longer than the adaxial epidermal cells (Table II; t test, $P = 7.0 \times 10^{-13}$ and $P = 1.1 \times 10^{-15}$, respectively).

Table I. *Apoplastic pH of cells expressing the PM H^+-ATPase compared with the apoplastic pH of nonexpressing cells*

Embryos were incubated in the culture medium supplemented with 30 μM IAA or in the culture medium without IAA for 1 h. They were then transferred to the dye containing culture medium supplemented with 30 μM IAA or not, respectively, for 75 min.

Adaxial Scutellar Epidermal Cells	−IAA		30 μMIAA	
	Wall pH	Ratio Mean	Wall pH	Ratio Mean
At the tip of the organ	5.5[a]	4.29 ± 0.57	4.65[c]	3.62 ± 0.20
Near the coleoptilar ring	5.75[b]	4.50 ± 0.51	5.25[d]	4.12 ± 0.43

[a]Fifty-eight ratio measurements were conducted on 13 embryos. [b]Fifty-seven ratio measurements have been performed on 10 embryos. [c]One hundred and eight ratio measurements have been conducted on 22 embryos. [d]One hundred and fifteen ratio measurements have been done on 20 embryos.

Table II. *Cell length determination along the scutellum epidermis of living embryos*

Cell length measurements based on cellulose staining of living non-sectioned embryos. Cell lengths of embryos of defined developmental stages were measured randomly. Due to experimental reasons, we measured either cell lengths on the adaxial or on the abaxial side of a given embryo. Nos. indicated in the table represent mean values followed by SDS.

Stages	Length of the Adaxial Epidermal Cells		Length of the Abaxial Epidermal Cells	
	μm			
Middle embryonic	23.1[a]	±5.6	40.3[b]	±10.6
Older embryonic	28.2[c]	±6.9	42.7[d]	±9.4

[a]The length of 29 cells that were spread over the adaxial epidermis of five embryos has been measured. [b]The length of 69 cells that were strewn over the distal abaxial epidermis of six embryos has been measured. [c]The length of 53 cells that were distributed over the adaxial epidermis of six embryos has been measured. [d]The length of 63 cells that were spread over the distal abaxial epidermis of six embryos has been measured.

DISCUSSION

In a previous study, an important accumulation of ^{3}[H],5-N_3IAA in the scutellum abaxial epidermis and at the tip of this organ was observed providing evidence for a transport toward the scutellum and indicating that these cells act as sink for the auxin analog (Fischer-Iglesias et al., 2001). In the present study, evidence was presented that these cells that act as sink for polarly transported auxin in bilaterally symmetrical embryos also express the PM H^+-ATPase. Besides correlation between the expression pattern of the PM H^+-ATPase and the distribution pattern of the auxin analog, [^{3}H],5-N_3IAA, western-blot analysis revealed that auxin increased the PM H^+-ATPase expression level by a factor 2 to 3 in wheat embryos. Furthermore, ratiometric analysis showed that the apoplastic pH of the cells expressing the PM H^+-ATPase was more acidic than the pH of nonexpressing cells. Finally, this acidification correlates with an increase of cell length in the scutellum abaxial epidermis.

Attainment of bilateral symmetry during early embryogenesis is achieved by the outgrowth laterally and axially of a shield-like shaped scutellum. Slightly deferred, the shoot apical meristem protrudes on the other side of the embryo proper. Auxin has been shown to play a role in the shift to bilateral symmetry and in the differentiation of meristems and scutellum. However, the mechanisms by which auxin acts during pattern formation are poorly understood. In this study, correlative evidence was provided for a role of the H^+-translocating ATPase as an auxin downstream target in the signaling cascade directing scutellum elongation. In particular, we propose that auxin augmented the rate of proton extrusion by increasing the amount of the proton pump in defined cells resulting in apoplastic acidification, a process contributing to the elongation of the scutellum.

No ATPase expression was detected in the embryo proper of globular embryos before scutellum differentiation, whereas in bilaterally symmetrical embryos, the PM H^+-ATPase antigen was restricted to the abaxial epidermis of the scutellum and to the distal tip of this organ. In morphological abnormal embryos whose auxin distribution or level were altered, a change in the expression pattern of PM H^+-ATPase was also observed. This expression pattern was specific for each type of morphological alteration and correlated to the distribution pattern of the azido-auxin. All of these data indicate that (a) the ATPase expression was induced in the cells containing significant levels of auxin, (b) manipulation of the auxin level or distribution resulted in ectopic expression of the ATPase in cells in which no detectable level of the protein was observed under normal conditions, or (c) both altered auxin distribution/level and altered PM H^+-ATPase spatial expression pattern were correlated to morphological abnormalities. In this respect, radial growth embryos are a representative example. In these ball-shaped embryos where no differentiation of the scutellum occurred, ATPase expression was observed in all epidermal cells around the radial embryo proper and in the internal cell layers. The absence of spatial restriction of the ATPase expression to defined cells may not

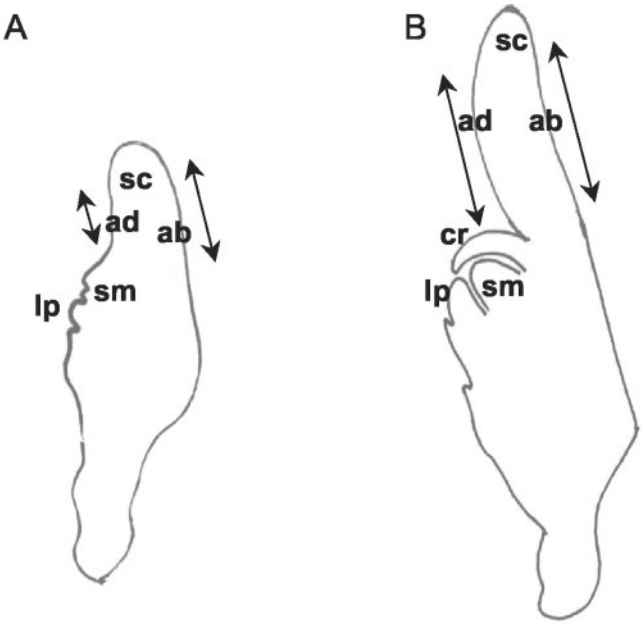

Figure 5. Plant material used to perform cell length measurement. Embryonic stages and localization of the epidermal cells used for measurements. A, Middle stage embryo whose first leaf primordium approximately covers one-half of the shoot meristem. B, Older embryo whose first leaf primordium covers the shoot meristem. ab, Abaxial scutellum epidermis; ad, adaxial scutellum epidermis; cr, coleoptilar ring; lp, first leaf primordium; sc, scutellum; sm, shoot meristem. Arrows indicate cell length measurement areas.

allow directed growth and normal scutellum differentiation. A change in the expression pattern of PM H^+-ATPase was also observed in auxin transport inhibitor-treated embryos. In particular, protein expression was observed in the elongation area between the shoot meristem and the scutellum of TIBA-treated embryos. This zone of cell hyperproliferation was not observed in control embryos and is specific for TIBA-treated embryos. Because the PM H^+-ATPase expression correlated with an accumulation of azido-IAA (Fischer-Iglesias et al., 2001), we suggest that important accumulation of auxin due to reduced polar transport may have increased the level of the proton pump leading to elongation between the shoot meristem and the suspensor.

Before the scutellum differentiates, no PM H^+-ATPase was detected by immunolocalization in the embryo proper of normal globular embryos, although the auxin analog was visualized in the epidermal cells and the inner cell layers. Two hypotheses may be proposed to explain this interesting finding. First, levels of auxin at the globular stage may be under the threshold required to achieve detectable PM H^+-ATPase expression in defined cells. Once a polar auxin transport takes place toward the developing scutellum and leads to an accumulation of the phytohormone in the scutellar epidermal and subepidermal cells, the levels of auxin may be sufficient to stimulate significantly PM H^+-ATPase expression in these cells. Second, transduction pathway(s) underlying initiation of scutellum elongation may require additional signaling molecules not available before the end of the globular stage to switch on the PM H^+-ATPase expression in defined cells.

The biochemical mechanism of cell wall loosening underlying elongation has not yet been elucidated and is matter of current debate. This process relies on the breakage or weakening of inter- or intramolecular load-bearing bonds within the chemically heterogeneous composite material of primary cell walls. The "acid growth theory" proposes that exposure of responsive cells to auxin leads to an increased rate of proton extrusion into the cell wall, presumably either by activation of the catalytic activity or by increasing the amount of PM H^+-ATPase protein, which results in a decreased apoplastic pH (Hager et al., 1971, 1991; Rayle and Cleland, 1977, 1992). The decreased pH of the cell wall induces "wall loosening" required for elongation. Other investigations have led to the identification of proteins such as xyloglucan endotransglycosylases and expansins that may also be involved in the regulation of cell wall extensibility by permitting the slippage between load-bearing microfibrils in the wall (Fry et al., 1992; Scherban et al., 1995; for review, see Cosgrove, 2000). Finally, Schopfer (2001) involved hydroxyl radicals as wall-loosening agents.

Although elongation is a process affecting a whole tissue or organ, the PM H^+-ATPase was mostly localized to the abaxial epidermal cells of the scutellum and to the adaxial epidermal cells at the distal tip of this organ, indicating a specific role of this cell layer in elongation. The notion that the epidermis mechanically limits growth and serves as a privileged tissue target for auxin action has become more and more entrenched in the literature, even though there is some kind of disagreement with this point of view (Rayle and Cleland, 1992). In particular, Kutschera (2001) reviewed the process of stem elongation and proposes the following theory that may also be pertinent for scutellum elongation. In an organ, the driving force for growth is provided by the thin-walled turgid inner tissues that have the tendency to spontaneously elongate under the action of cell turgor pressure, whereas the rate of elongation is regulated by loosening and stiffening events restricted to the peripheral walls. Different cell wall architecture is largely responsible for these properties. The outer epidermal walls of an organ have an helicoidal cellulose architecture with microfibrils oriented in both longitudinal and transverse directions. In contrast, the thin walls of the inner tissues are unilayered with cellulose microfibrils preferentially oriented in transverse direction with respect to the axis of elongation. The concept of cell wall loosening is only relevant for the growth-limiting thick walls. Thus, wall-loosening processes may permit the slippage between load-bearing bonds in the thick walls. The resulting stress relaxation within these thick walls may enhance their ability to become irreversibly extended under the force of turgor pressure exerted by the thin-walled internal tissues of the organ. An intriguing open question is whether this concept may apply to scutellum elongation too.

There is no agreement about the value of cell wall pH that triggers wall extension under natural conditions (Grignon and Sentenac, 1991). Threshold for normal auxin dependant growth of stems and coleoptiles has been reported to be pH 5 to 5.25 (Metraux and Taiz, 1977; Schopfer, 1993; Kutschera, 2001), and ratiometric measurements applied to cells of the elongation zone of corn roots revealed an apoplastic pH of 4.9 (Taylor et al., 1996).

Ratiometric confocal imaging was used to test whether the expression of H^+-ATPase in defined cells leads to localized pH changes within the embryo. Confocal laser scanning microscopy allows precise pH measurement with a sensitivity of approximately 0.2 pH units at defined spatial locations in living tissues. This approach has been mostly used to measure cytoplasmic pH (Hepler and Gunnings, 1998). It has more recently also been used for measurements of apoplastic pH in roots or root hairs (Taylor et al., 1996; Bibikova et al., 1998; Yu et al., 2001). To our knowledge, this is the first time that this technique was applied to embryos. When exogenous auxin was added to the embryos, albeit the apoplastic pH of the entire epidermis of the scutellum was relatively acidic, cells expressing the

ATPase such as those on the tip of the scutellum had a clearly more acidic wall pH (4.65) compared with the epidermal cells closer to the coleoptile in which the ATPase was not expressed (pH 5.25). Apoplastic pH was also measured in the absence of exogenously added auxin. However, in this case, it has to be mentioned that there is a significant auxin leakage in the culture medium (Fischer-Iglesias et al., 2001). Therefore, the apoplastic pH value of cells at the tip of the scutellum may be underestimated because PM H^+-ATPase amounts were dependent on auxin concentration. This may also explain why no pH gradient was observed in between the cells of the two embryonic areas. On the other hand, the apoplastic pH of cells close to the coleoptilar ring of IAA-treated embryos was more acidic ($\Delta pH \approx 0.5$) than the wall pH of the corresponding cells of non-treated embryos even though neither auxin nor the proton pump were detected in these cells under normal conditions. In this case, the exogenous auxin may have increased the amount of PM H^+-ATPase in cells that under normal conditions did not contain detectable levels of the protein augmenting the capacity of the membranes for proton export. Therefore, the physiological apoplastic pH of these cells may not be as acidic as the value measured under these experimental conditions. Such a mechanism may have occurred in radial-growth embryos subjected over a longer time period to IAA treatment as suggested by the overall expression of the PM H^+-ATPase in the radial embryo proper. In conclusion, although some of these pH values may not be taken as absolute wall pH values in planta, the measurements performed clearly showed that there was an apoplastic pH gradient in the embryo along the scutellum epidermis.

Close inspection of scutellum epidermis cells shows some heterogeneity in wall pH. The source of this variability is unknown but may reflect natural microdomains of altered apoplastic pH due to the complex structure of the wall or to localized wall-loosening activity.

Coleoptiles are the experimental system that provided most of the data on auxin-induced acidification together with stems (Kutschera, 2001). Coleoptiles grow exclusively by elongation in contrast to scutella, which grow also by cell multiplication. Although some investigations did not reveal any auxin-induced increase in the amount of PM H^+-ATPase in maize coleoptiles (Jahn et al., 1996), many other studies performed, in particular by Frias et al. (1996), showed that the mRNA of a major isoform of the maize PM H^+-ATPase (MHA2) was induced when nonvascular parts of coleoptile segments were treated with auxin. This induction correlates with auxin-triggered proton extrusion and with elongation by the same part of the segment. Interestingly, the highest expression of MHA2 transcripts was also detected in the maize embryo in the scutellar epidermal cells facing the endosperm (Frias et al., 1996).

Selective inhibition of the PM-H^+ATPase and analysis of the effect of such an inhibition on the establishment of bilateral symmetry and differentiation of the scutellum was not possible to date because orthovanadate, the most commonly used inhibitor of PM H^+-ATPase, affects also auxin polar transport (W. Michalke, personal communication).

Finally, it should be mentioned that the PM H^+-ATPase represents an excellent marker for the scutellum, in particular for the epidermal cells of this organ, and therefore the identification of this marker opens new perspectives for other studies on embryo development.

CONCLUSIONS

This study provided new insights into the auxin transduction pathway(s) that may direct pattern formation in embryos by the identification of essential components of the signaling cascade implicated in cell wall loosening and organ elongation. In summary, we propose a model in which auxin polar transport in bilaterally symmetrical embryos leads to an accumulation of the hormone in epidermal cells of the scutellum. In the latter cells, auxin increased the H^+-ATPase expression level required to augment the capacity of the membranes for proton export. The resulting lowering of pH is proposed to be involved in cell wall-loosening processes required for directed cell elongation and growing of the scutellum during embryo development.

MATERIALS AND METHODS

Plant Material

Wheat (*Triticum aestivum* L. cv Sonora) plants were grown as described by Fischer et al. (1997). Immature ears were collected 3 to 13 d after anthesis and were sterilized with 70% (v/v) ethanol for 1 min. In vitro culture of embryos was performed as described by Fischer and Neuhaus (1995, 1996) and by Fischer et al. (1997)).

For preparation of microsome vesicles, wheat and corn (*Zea mays*) seedlings were grown for 5 d at 25°C in the dark with two pulses of red light at d 3 and 4. Arabidopsis (Landsberg *erecta*) plants were grown for 6 weeks in long-day conditions (16 h at 22°C in the light and 8 h at 18°C in the dark).

Immunolocalization

Fixation of wheat embryos for immunolocalization was carried out overnight at room temperature in PHEMS buffer (60 mM PIPES, 25 mM HEPES, 10 mM EGTA, and 2 mM $MgCl_2$, pH 6.9) containing 3.7% (w/v) paraformaldehyde. After washing in distilled water, the samples were dehydrated in a graded ethanol series and then embedded in Steedman's wax (polyethyleneglycol distearate:hexadecanol [9:1, v/v]).

Eight- to 10-μm sections were performed with a microtome (Leica, Wetzlar, Germany) and mounted with 0.5% (w/v) gelatine (Merck, Darmstadt, Germany) on slides covered with a acetone solution containing 8% (v/v) 3-aminopropyltriethoxysilane (Fluka, Buchs, Switzerland). After dewaxing in isopropanol, samples were rehydrated through an ethanol series. A second fixation step was carried out with 3.7% (w/v) paraformaldehyde in phosphate-buffered saline (PBS; 135 mM NaCl, 24 mM KCl, 7.9 mM Na_2HPO_4, and 1.5 mM KH_2PO_4, pH 7.2) for 5 min at 4°C. Endogenous peroxidases were inactivated by incubating the sections in a PBS:methanol (1:1, v/v) solution containing 0.3% (v/v) H_2O_2 for 30 to 40 min at room temperature. Unspecific sites were saturated by incubation in PBS contain-

ing 0.2% (v/v) Tween 20 containing 4% (w/v) bovine serum albumin (BSA) for at least 30 min. Immunoreaction occurred overnight at 4°C with 1:50-diluted H^+-ATPase antibody in PBS containing 0.2% (v/v) Tween 20 containing 4% (w/v) BSA. The monoclonal 46E5B11 antibody used in this study was originally raised against the maize PM H^+-ATPase (Villalba et al., 1991). The second blocking step was carried out with normal serum from horse for approximately 60 min at room temperature according to the instructions provided by the Vectastain ABC-Kit Elite (Vector Laboratories, Burlingame, CA). Incubation with the secondary antibody, a biotinylated horse anti-mouse IgG, and the staining procedure were also performed according to the supplier's instructions (Vectastain ABC-Kit Elite). Sections were air-dried, mounted in vitro-Clud (Langenbrinck, Emmendingen, Germany), and observed using an Axioplan microscope (Carl Zeiss, Oberkochen, Germany).

Preparation of PM-Enriched Microsomes

Coleoptiles together with primary leaf and parts of mesocotyl were harvested from corn and wheat seedlings. The inflorescences including stems without the leaf rosettes were harvested from Arabidopsis plants. PM-enriched microsomes were prepared from this plant material according to the method described by Thein and Michalke (1988) with slight modifications. The plant material was homogenized in extraction buffer (300 mM NaCl, 20 mM Tris, 20 mM EDTA, 2% (w/v) polyvinylpyrrolidon, pH 8; 1% (w/v) BSA, 20 mM dithiothreitol, and 0.5 mM phenylmethylsulfonylfluoride were freshly added before homogenization), filtered through a nylon cloth, and centrifuged at 2,600*g* for 25 min. Microsomes from the supernatant were sedimented at 90,000*g* for 45 min and resuspended in extraction buffer (without polyvinylpyrrolidon and without the freshly added substances). From this suspension, inner membranes and inside out plasma membranes were precipitated using 4.4% (w/v) polyethyleneglycol. The right-side out plasma membranes enriched in the supernatant were sedimented at 90,000*g* for 45 min and resuspended as desired.

Western-Blot Analysis

Immature wheat embryos were isolated out of the kernels and incubated for 2 h at room temperature in Murashige and Skoog (1962) liquid medium containing 3% (w/v) Suc either supplemented with 30 μM IAA or without IAA (control).

Protein concentrations of total extracts were determined according to Bradford (1976), and equal amounts of protein extracted from treated and non-treated embryos were separated by electrophoresis on SDS-PAGE gels as described by Laemmli (1970). Proteins were electrotransferred to PVDF membranes using a Transblot SD apparatus (Bio-Rad, Hercules, CA) following the "semidry"-method (Ausubel et al., 1997). Ponceau Red staining was performed to verify that same amounts of protein from treated and non-treated embryo extracts were transferred to the membrane. Blocking of aspecific binding was performed with 5% (w/v) low-fat milk powder in Tris-buffered saline for 1 h at room temperature. The blots were exposed to the anti-ATPase antibody (diluted 1:500) for 1 h and 30 min at room temperature. Signal detection was achieved using peroxidase-conjugated anti-mouse IgG followed by a chemiluminescence reaction (ECL-system, Amersham Biosciences AB, Uppsala) and exposure to x-ray film for 10 s to 15 min. Western-blot analysis was performed on PM-enriched microsomal preparations of Arabidopsis, maize, and wheat following the same procedure.

Electron Microscopy

Isolated wheat embryos were fixed in 4% (w/v) formaldehyde and 0.1% (w/v) glutaraldehyde in cacodylate-buffer, dehydrated in alcohol, and embedded in Lowicryl K4M resin. Immunolabeling was carried out using a PBS solution (pH 7.2) containing 1% (w/v) BSA (Dianova, Hamburg, Germany) and 0.1% (v/v) Tween 20 (Serva, Heidelberg). The anti-ATPase antibody (46E5B11) was diluted 1:100 in the PBS. The second antibody, goat anti-mouse IgG, gold-coupled with a particle size of 10 nm (Dianova), was diluted 1:20 in labeling buffer. Electron microscopy was carried out using an electron microscope (CM 10, Philips, Kassel, Germany) at 60 kV.

Imaging of Wall pH in Wheat Embryo

Epidermal cell wall pH of scutellum was monitored by pseudoratiometric confocal imaging of the fluorescence emitted by the pH-sensitive dye OG 488 conjugated to a 10,000 M_r dextran (pK = 4.7), and by the pH-insensitive dye TR conjugated to a dextran of 10,000 M_r as an internal standard (Molecular Probes, Eugene, OR). The ratiometric approach allows elimination of artifacts caused by uneven distribution, photobleaching, and leakage of the dye from cell walls and compensation for variations in loading. The dyes were added to the culture medium of the embryos at concentrations of 80 and 300 μM, respectively. This culture medium was a modified N6 medium (Fischer and Neuhaus, 1995) containing 5% (w/v) Suc and 25 mM MES, pH 6. The OG/TR signal was calibrated to wall pH using a modified N6 medium supplemented with 80 μM OG and 300 μM TR buffered either with 25 mM MES to pH range of 5.3 to 6.5 or with 25 mM citrate to pHs ranging from 3.6 to 4.7. For in situ calibration, embryos were killed by freezing/thawing and then incubated for 75 min in the dye containing culture medium adjusted to the different pHs. After washing, they were observed in the respective culture media devoid of dyes. For measurements of epidermal cell wall pH, freshly excised embryos were preincubated in the culture medium supplemented with 30 μM IAA or in the culture medium free of IAA for 1 h. The embryos were then transferred to the dye containing culture medium supplemented or not with 30 μM IAA for 75 min. After washing, the embryos were mounted in the culture medium devoid of dyes, supplemented or not with IAA for immediate observation to avoid leakage of the dyes. Wall pH was imaged with a Leica TCS 4D confocal laser scanning unit attached to a fluorescent microscope (RM Rbe, Leitz, Midland, Ontario). To collect pseudoratio images, excitation at 488 line of a Ar/Kr laser was used, and emission was detected at 515 to 580 nm for OG and at >590 nm for TR.

Determination of the Cell Size

The length of the cells of the scutellum adaxial epidermis were compared with the length of the scutellum abaxial epidermal cells (Fig. 5). Two different embryonic stages were used, namely bilaterally symmetrical embryos whose first leaf primordium covered approximately one-half of the shoot meristem (middle embryonic stages; Fig. 5) and slightly older embryos whose first leaf primordium covered the shoot meristem (older embryonic stages; Fig. 5).

Numerous living in planta grown embryos isolated right before treatment were dipped for 10 min in the culture medium (modified N6 medium with 5% [w/v] Suc and 25 mM MES, pH 5.6) containing 0.5% (w/v) Primuline (Aldrich Chemical Co., Milwaukee), a cellulose specific fluorescent dye. After washing, the embryos were observed in the culture medium using a Axioplan microscope (Carl Zeiss; Table II).

ACKNOWLEDGMENT

We thank Rainer Hertel for critical reading of the manuscript.

Received August 23, 2002; returned for revision October 3, 2002; accepted December 11, 2002.

LITERATURE CITED

Ausubel FM, Brent R, Kingston RE, Moore DD, Seidmann JG, Smith JA, Struhl K, editors (1997) Current Protocols in Molecular Biology, Vol 1–3. John Wiley & Sons, New York

Baur M, Meyer AJ, Heumann H-G, Lützelschwab M, Michalke W (1996) Distribution of plasma membrane H^+-ATPase and polar current patterns in leaves and stems of *Elodea canadensis*. Bot Acta **109:** 382–387

Berleth T, Jürgens G (1993) The role of the *MONOPTEROS* gene in organizing the basal body region of the *Arabidopsis* embryo. Development **118:** 575–587

Bibikova TN, Jacob T, Dahse I, Gilroy S (1998) Localized changes in apoplastic and cytoplasmic pH are associated with root hair development in *Arabidopsis thaliana*. Development **125:** 2925–2934

Bouche-Pillon S, Fleurat-Lessard P, Serrano R, Bonnemain J-L (1994) Asymmetric distribution of the plasma-membrane H^+-ATPase in embryos of *Vicia faba* L. with special reference to transfer cells. Planta **193:** 392–397

Bradford MM (1976) A rapid and sensitive method for the quantification of microgram quantities of protein utilizing the principle of protein dye-binding. Anal Biochem **72:** 248–254

Christensen SK, Dagenais N, Chory J, Weigel D (2000) Regulation of auxin response by the protein kinase PINOID. Cell **100:** 469–478

Cosgrove DJ (2000) Loosening of plant cell walls by expansins. Nature **407:** 321–326

Del Pozo JC, Timpte C, Tan S, Callis J, Estelle M (1998) The ubiquitin-related protein RUB1 and auxin response in *Arabidopsis*. Science **280:** 1760–1763

El Ayadi R (1987) Propriétés et méchanismes de l'absorption des glucides par les embryons de *Vicia faba* L. PhD thesis. Poitiers University, France

Endrizzi K, Moussian B, Haecker A, Levin JZ, Laux T (1996) The *SHOOT MERISTEMLESS* gene is required for maintenance of undifferentiated cells in *Arabidopsis* shoot and floral meristems and acts at a different regulatory level than the meristem genes *WUSCHEL* and *ZWILLE*. Plant J **10:** 967–979

Ewing NN, Bennett AB (1994) Assessment of the number and expression of P-type H^+-ATPase genes in tomato. Plant Physiol **106:** 547–557

Fischer C, Neuhaus G (1995) *In vitro* development of globular zygotic wheat embryos. Plant Cell Rep **15:** 186–191

Fischer C, Neuhaus G (1996) Influence of auxin on the establishment of bilateral symmetry in monocots. Plant J **9:** 659–669

Fischer C, Speth V, Fleig-Eberenz S, Neuhaus G (1997) Induction of zygotic polyembryos in wheat: influence of auxin polar transport. Plant Cell **9:** 1767–1780

Fischer-Iglesias C, Sundberg B, Neuhaus G, Jones AM (2001) Auxin distribution and transport during embryonic pattern formation in wheat. Plant J **26:** 115–129

Frias I, Caldeira MT, Perez-Castineira JR, Navarro-Avino JP, Culianez-Macia FA, Kuppinger O, Stransky H, Pages M, Hager A, Serrano R (1996) A major isoform of the maize plasmamembrane H^+-ATPase: characterization and induction by auxin in coleoptiles. Plant Cell **8:** 1533–1544

Fry SC, Smith RC, Renwick KF, Martin DJ, Hodge SK, Matthews KJ (1992) Xyloglucan endotransglycosylase, a new wall-loosening enzyme activity from plants. Biochemical J **282:** 821–828

Gray WM, del Pozo JC, Walker L, Hobbie L, Risseeuw E, Banks T, Crosby WL, Yang M, Ma H, Estelle M (1999) Identification of an SCF ubiquitin-ligase complex required for auxin response in *Arabidopsis thaliana*. Genes Dev **13:** 1678–1691

Grignon C, Sentenac H (1991) pH and ionic conditions in the apoplast. Annu Rev Plant Physiol Plant Mol Biol **42:** 103–128

Guilfoyle TJ, Hagen G (2001) Auxin response factors. J Plant Growth Regul **20:** 281–291

Hadfi K, Speth V, Neuhaus G (1998) Auxin-induced developmental patterns in *Brassica juncea* embryos. Development **125:** 879–887

Hager A, Debus G, Edel H-G, Stransky H, Serrano R (1991) Auxin induces exocytosis and the rapid synthesis of a high-turnover pool of plasmamembrane H^+-ATPase. Planta **185:** 527–537

Hager A, Menzel H, Krauss A (1971) Versuche und Hypothese zur Primärwirkung des Auxins beim Streckungswachstum. Planta **100:** 47–75

Hamann T, Benkova E, Baurle I, Kientz M, Jürgens G (2002) The *Arabidopsis* BODENLOS gene encodes an auxin response protein inhibiting MONOPTEROS-mediated embryo patterning. Genes Dev **16:** 1610–1615

Hardtke CS, Berleth T (1998) The *Arabidopsis* gene *MONOPTEROS* encodes a transcription factor mediating embryo axis formation and vascular development. EMBO J **17:** 1405–1411

Hepler PK, Gunnings BES (1998) Confocal fluorescence microscopy of plant cells. Protoplasma **201:** 121–157

Jahn T, Baluska F, Michalke W, Harper JF, Volkmann D (1998) A membrane H^+-ATPase in the root apex: evidence for strong expression in xylem parenchyma and asymmetric localization within cortical and epidermal cells. Physiol Plant **104:** 311–316

Jahn T, Johansson F, Lüthen H, Volkmann D, Larsson C (1996) Reinvestigation of auxin and fusicoccin stimulation of the plasma-membrane H^+-ATPase activity. Planta **199:** 359–365

Jürgens G, Mayer U, Torres Ruiz RA, Berleth T, Misera S (1991) Genetic analysis of pattern formation in the *Arabidopsis* embryo. Development Suppl **1:** 27–38

Kovtun Y, Wan-Ling C, Weike Z, Sheen J (1998) Suppression of auxin signal transduction by a MAPK cascade in higher plants. Nature **395:** 716–720

Kutschera U (2001) Stem elongation and cell wall proteins in flowering plants. Plant Biol **3:** 466–480

Laemmli UK (1970) Cleavage of structural proteins during the assembly of the head of bacteriophage T4. Nature **227:** 680–685

Leyser O (2001) Auxin signalling: the beginning, the middle and the end. Curr Opin Plant Biol **4:** 382–386

Liu C, Xu Z, Chua N (1993) Auxin polar transport is essential for the establishment of bilateral symmetry during early plant embryogenesis. Plant Cell **5:** 621–630

Lyapina S, Cope G, Shevchenko A, Serino G, Tsuge T, Zhou C, Wolf DA, Wei N, Shevchenko A, Deshaies R (2001) Promotion of NEDD8-CUL1 conjugate cleavage by COP9 signalosome. Science **292:** 1382–1385

Mayer U, Büttner G, Jürgens G (1993) Apical-basal pattern formation in the Arabidopsis embryo: studies on the role of the GNOM gene. Development **117:** 149–162

Mayer U, Torres Ruiz RA, Berleth T, Misera S, Jürgens G (1991) Mutations affecting body organization in the *Arabidopsis* embryo. Nature **353:** 402–407

Metraux JP, Taiz L (1977) Cell wall extension in *Nitella* is influenced by acids and ions. Proc Natl Acad Sci USA **74:** 1565–1569

Murashige T, Skoog F (1962) A revised medium for rapid growth and bioassays with tobacco tissue culture. Physiol Plant **15:** 473–497

Palmgren MG, Christensen G (1994) Functional comparisons of plant plasma membrane H^+-ATPase isoforms expressed in yeast. J Biol Chem **269:** 3027–3333

Rayle DL, Cleland RE (1977) Control of plant cell enlargement by hydrogen ions. Curr Top Dev Biol **11:** 187–214

Rayle DL, Cleland RE (1992) The acid growth theory of auxin-induced cell elongation is alive and well. Plant Physiol **99:** 1271–1274

Reed JW (2001) Roles and activities of Aux/IAA proteins in *Arabidopsis*. Trends Plant Sci **6:** 420–425

Ruegger M, Dewey E, Gray WM, Hobbie L, Turner J, Estelle M (1998) The TIR1 protein of *Arabidopsis* functions in auxin response and is related to human SKP2 and yeast Grr1p. Genes Dev **12:** 198–207

Scherban TY, Shi J, Durachko DM, Guiltinan MJ, McQueen-Mason SJ, Shie M, Cosgrove DJ (1995) Molecular cloning and sequence analysis of expansins, a highly conserved multigene family of proteins that mediate cell wall extension in plants. Proc Natl Acad Sci USA **92:** 9245–9249

Schiavone FM, Cooke TJ (1987) Unusual patterns of somatic embryogenesis in the domesticated carrot: developmental effects of exogenous auxins and auxin transport inhibitors. Cell Differ **21:** 53–62

Schopfer P (1993) Determination of auxin-dependent pH changes in coleoptile cell walls by null point method. Plant Physiol **103:** 351–357

Schopfer P (2001) Hydroxyl radical-induced cell wall loosening *in vitro* and in *vivo*: implication for the control of elongation growth. Plant J **28:** 679–688

Schwechheimer C, Serino G, Callis J, Crosby WL, Lyapina S, Deshaies RJ, Gray WM, Estelle M, Deng X-W (2001) Interactions of the COP9 signalosome with the E3 ubiquitin ligase SCF^{TIR} in mediating auxin response. Science **292:** 1379–1382

Serrano R (1989) Structure and function of plasma membrane H(+) ATPase. FEBS Lett **325:** 108–111

Sessions AR, Nemhauser JL, McColl A, Roe J, Feldman KA, Zambryski PC (1997) *ETTIN* patterns the *Arabidopsis* floral meristem and reproductive organs. Development **124:** 4481–4491

Sussman MR (1994) Molecular analysis of proteins in the plant plasma membrane. Annu Rev Plant Physiol Plant Mol Biol **40:** 61–94

Taylor DP, Slattery J, Leopold AC (1996) Apoplastic pH in corn root gravitropism: a laser scanning confocal microscopy measurement. Physiol Plant **97:** 35–38

Thein M, Michalke W (1988) Bisulfite interacts with binding sites of the auxin-transport inhibitor *N*-1naphthylphthalamic acid. Planta **176:** 343–350

Torres-Ruiz RA, Lohner A, Jürgens G (1996) The GURKE gene is required for normal organization of the apical region in the *Arabidopsis* embryo. Plant J **10:** 1005–1016

Ulmasov T, Hagen G, Guilfoyle TJ (1997a) ARF1, a transcription factor that binds auxin response elements. Science **276:** 1865–1868

Ulmasov T, Murfett J, Hagen G, Guilfoyle TJ (1997b) Aux/IAA proteins repress expression of reporter genes containing natural and highly active synthetic auxin response elements. Plant Cell **9:** 1963–1971

Villalba JM, Lützelschwab M, Serrano R (1991) Immunocytolocalization of plasma-membrane H^+-ATPase in maize coleoptiles and enclosed leaves. Planta **185:** 458–461

Ward SP, Estelle M (2001) Auxin signalling involves regulated protein degradation by the ubiquitin-proteasome pathway. J Plant Growth Regul **20:** 265–273

Yu Q, Kuo J, Tang C (2001) Using confocal laser scanning microscopy to measure apoplastic pH change in roots of *Lupinus angustifolius* L. in response to high pH. Ann Bot **87:** 47–52